Explosive tephra emissions at Mount St. Helens, 1989–1991: The violent escape of magmatic gas following storms?

LARRY G. MASTIN *U.S. Geological Survey, Cascades Volcano Observatory, 5400 MacArthur Boulevard, Vancouver, Washington 98661*

ABSTRACT

From 24 August 1989 until 18 June 1991, Mount St. Helens produced at least 28 shallow, explosion-like seismic events with signatures similar to those produced by gas explosions on the dome during the mid 1980s. At least six were accompanied by violent emission of non-juvenile tephra, ejection of blocks of rock nearly 1 km from the vent, and avalanching of debris off the north side of the dome. Four produced no emission of tephra, and the remainder occurred when the crater could not be observed (although later crater visits found no new tephra deposits). All six confirmed emissions and most (although not all) other seismic events took place hours to days after storms. Over time periods ranging from 2 to 15 days, statistical goodness of fit tests give a probability of 1×10^{-2} to 1×10^{-5} that the precipitation prior to emissions was fortuitously greater than normal. Similar tests for precipitation prior to all 28 events give probabilities of 3×10^{-2} to 1×10^{-3}. The short delay between storms and emissions suggests that the events that follow storms originate at very shallow depth, probably within the dome itself. Although the exact causal mechanism is not known, it is speculated that slope instability or accelerated growth of cooling fractures following storms may have released gas trapped within or at the base of the dome. Of the events that did not follow storms, three were located seismically between 1.4 and 2.1 km depth. Thus the events as a group are not confined to shallow depth and probably record gas transport from a deeper, magmatic source. A deep source is also suggested by an unprecedented, 4-yr-long increase in background seismicity at 2- to 9-km depth that peaked in 1989 and 1990. Calculations indicate that the energy content of gas exsolved from the crystallizing conduit was probably sufficient to power the emissions.

INTRODUCTION

In the spring of 1980, Mount St. Helens in southwestern Washington State (Fig. 1), began a decade-long period of eruptive activity that has been among the most extensively documented of any eruptive sequence (for example, Lipman and Mullineaux, 1981; Pallister and others, 1992). The activity included six major Plinian eruptions in 1980, followed by six years of dome growth from October 1980 to October 1986. From October 1986 until mid-1989, Mount St. Helens was relatively quiet. On 24 August 1989, however, Mount St. Helens was rocked again by a shallow seismic event strikingly similar to signals of the early and mid-1980s that had accompanied explosive emissions of steam and ash (Jonientz-Trisler and others, 1991). From August 1989 until June 1991, there followed at least 27 more shallow, explosion-like seismic events of this type. At least six produced violent emissions of gas (mostly steam) and tephra, showers of ballistically ejected blocks that covered the crater floor, and small debris flows that traveled down the Toutle River Valley.

Small gas explosions of this type in the past have not been especially well documented or their triggering mechanisms well understood, but recent deaths at Galeras Volcano, Colombia, and Guagua Pichincha, Ecuador, from eruptions of this type (Kerr, 1993) demonstrate the need to understand and predict them. The emissions at Mount St. Helens show important similarities to the eruptions at Galeras and Guagua Pichincha in two respects: as at Galeras (Kerr, 1993), volatile exsolution from magma is a plausible source of gas for these events; as at Guagua Pichincha (Smithsonian Institution, 1993), the emissions at Mount St. Helens are associated with periods of wet weather. Although associations between gas or steam explosions and rainfall have been mentioned in past studies (for example, McBirney, 1955; Murray, 1980), this is the first case known to this author where such a correlation has been statistically documented. This paper describes these events and interprets their cause.

DESCRIPTION OF THE EVENTS

In contrast to the magmatic eruptions of the early and mid-1980s (Chadwick and others, 1983; Dzurisin and others, 1983; Swanson and others, 1983), the shallow, explosion-like seismic events of August 1989 and later had no apparent short-term precursors. Seismicity at 2- to 9-km depth below the crater had been increasing gradually since late 1987 (Moran, in press), but did not deviate significantly from this trend in the days or weeks preceding any of the events. Tiltmeters and repeated geodetic surveys also recorded no uplift of the crater floor or other deformation that could be intrusion-related.

The onsets to the seismic events ranged from emergent to abrupt. Within the crater, each was characterized by continuous, high-amplitude shaking of medium frequency (for example, 5–7 Hz for the 24 August 1989 event) that lasted from less than a minute to several hours (Fig. 2; Table 1). The signatures are quite different from discrete, seconds-long monochromatic ~0.5-Hz signals inferred to be caused by gas transport at Redoubt Volcano (Chouet and others, in press). The shaking was followed for minutes to hours by many, small, high-frequency earthquakes, at the rate of a few per minute to one every few minutes. One emission event, on 20 December 1990, was followed for more than two weeks by several hundred small-magnitude earthquakes, located below or just north of the dome. Those occurring in the first few days were all less than 3 km below the base of the dome, but later ones ranged to more than 5 km (S. C. Moran, 1992, written commun.).

The long duration and high amplitude of the signal, and the sequence of small earthquakes in the latter part of the record distinguished shallow, explosion-like seismicity

Geological Society of America Bulletin, v. 106, p. 175–185, 10 figs., 3 tables, February 1994.

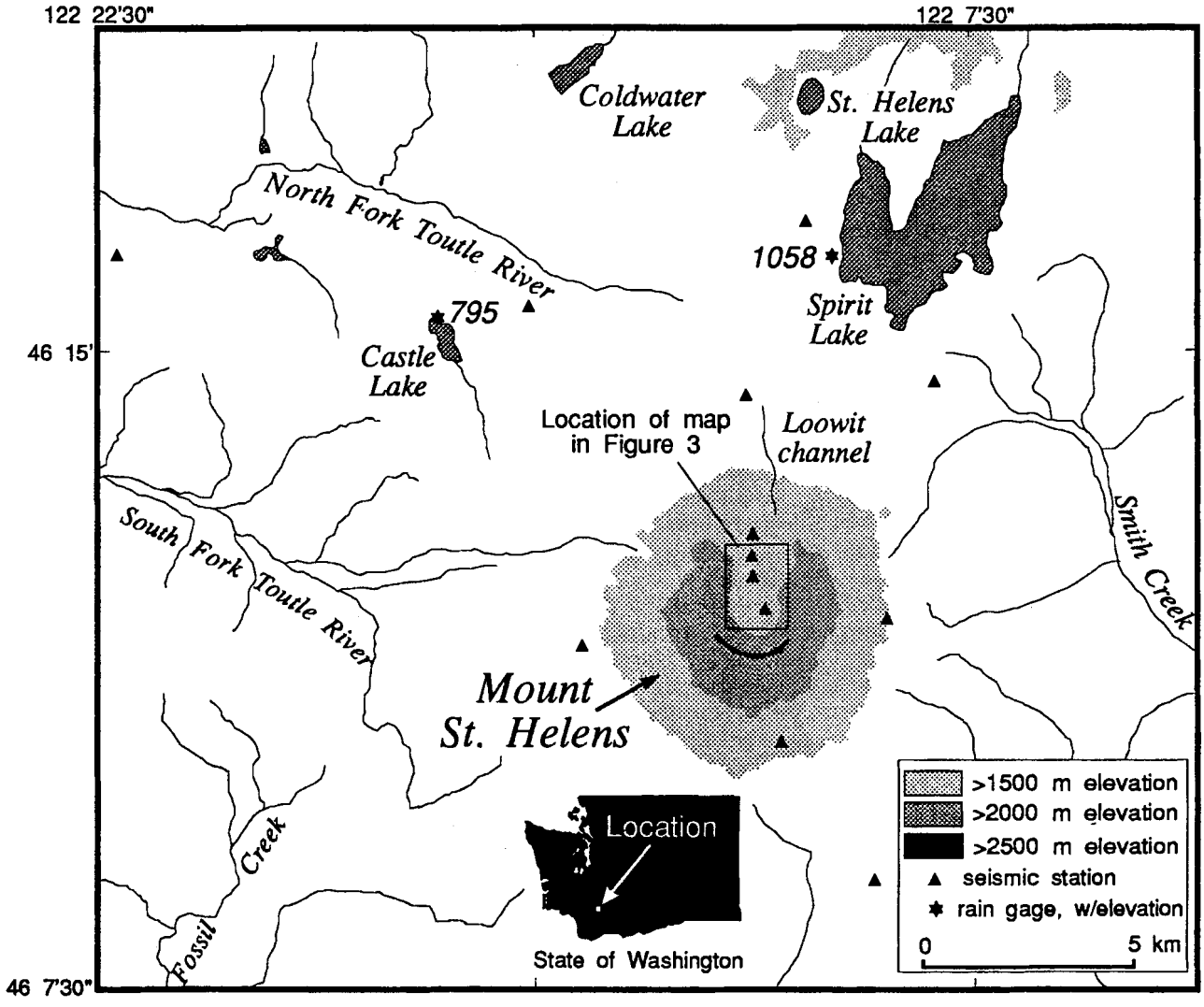

Figure 1. Map of the Mount St. Helens area.

from the rumbling of rock fall, the buffeting of the stations by wind, and the sharp arrivals and rapid exponential decay (within seconds) of earthquakes that typify the Mount St. Helens magmatic system (Jonientz-Trisler and others, 1991). Strong shaking was generally confined to the crater, suggesting that the source was shallow.

Blasts from five of the six confirmed emissions issued in a northward direction from a vent on the north shoulder of the lava dome (NV, Fig. 3). This area overlies a normal fault scarp on the crater floor that channeled gas to the surface (as shown, for example, in Fig. 2 of Chadwick and Swanson, 1989) before it was covered by lava and rock-avalanche debris. One small event (on 20 December 1990) issued from a point on the northeast shoulder of the dome (EV, Fig. 3), and one (on 5 February 1991; Fig. 4) appeared to have issued from both vents simultaneously. The largest blasts ballistically ejected dacite blocks 0.5–1.0 m in diameter (b, Fig. 4) up to 1 km north of the vent, suggesting ejection velocities of several tens of meters per second to more than 100 m per second based on ballistic relations described in Mastin (1991). Average velocities were probably somewhat less (perhaps 40–80 m/s). Accompanying or following these blasts were small ash-cloud surges (producing deposit ac, Fig. 4) and poorly inflated lithic gravity-driven flows that poured off the dome. Traces of ash were occasionally blown by high winds as far as 140 km from the mountain, and white steam plumes were reported by airline pilots as high as 5.5 km above the dome (perhaps an overestimate). Mixtures of ejecta and melted snow frequently mobilized into small debris flows (df, Fig. 4) that propagated northward out of the crater.

The deposits consist of lithic dacite from the dome, with a small amount (<1%) of dark, glassy, high-silica andesite or low-silica dacite that may represent the early (1981) interior of the dome or the conduit (Pallister and others, 1992). No debris from below the base of the dome has been found, although a significant fraction of debris (>10%) is unidentified and may include sub-domal fragments. There is no evidence of juvenile glass in any debris.

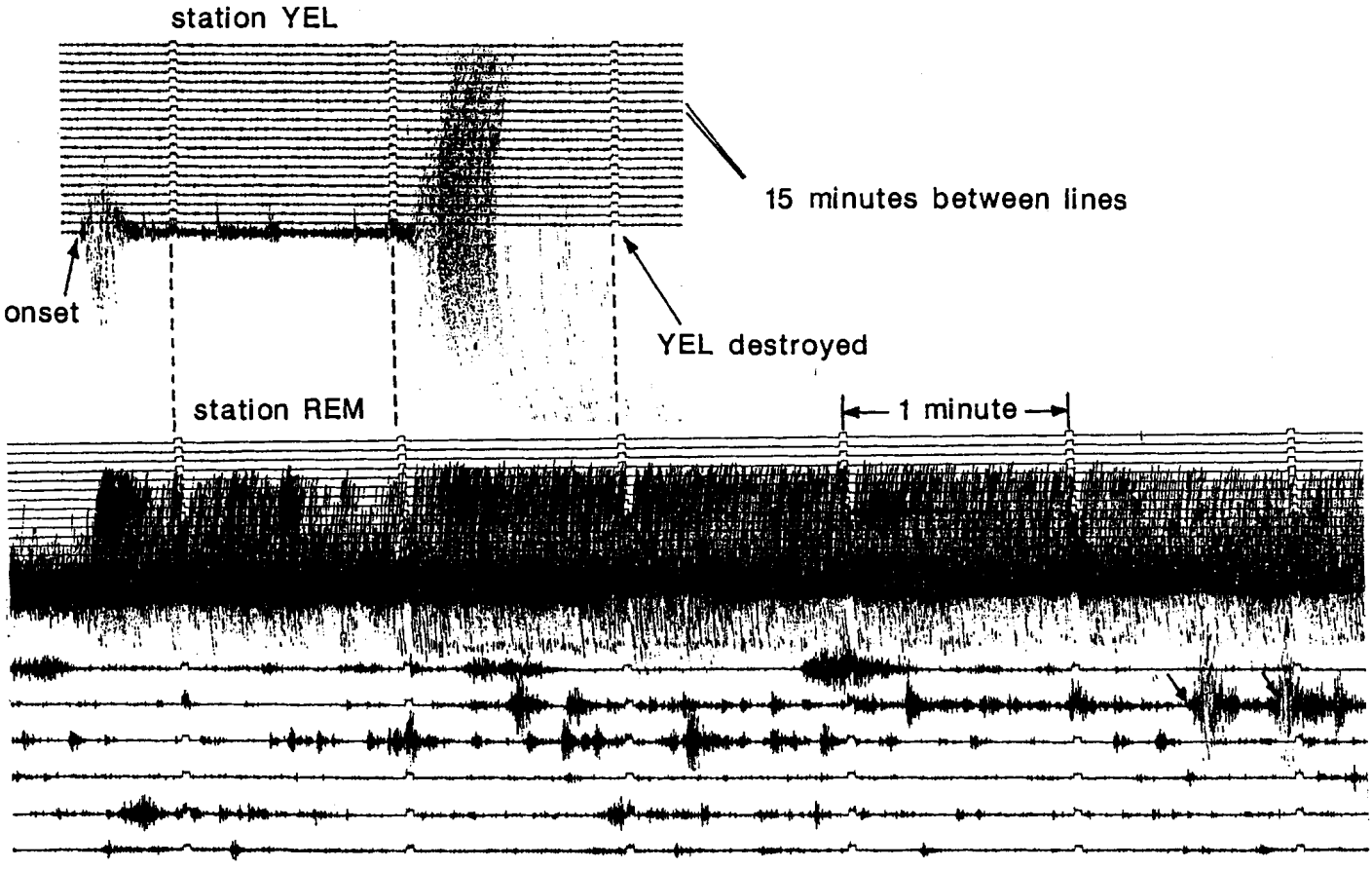

Figure 2. Seismograms of the 5 November 1990, event from the stations Yellow Rock (YEL) and Rembrandt (REM). Locations of seismic stations shown in Figure 3.

CORRELATION WITH PRECIPITATION: THE EVIDENCE FOR A SHALLOW TRIGGER

In 1990, some workers (J. Costa, R. LaHusen) at the Cascades Volcano Observatory observed a coincidence in timing between emissions and major storms. To see if this coincidence was significant, data from three tipping-bucket–type rain gages near Mount St. Helens were analyzed for the period 16 August 1989 through 30 June 1991. These gages register rainfall in 0.01-in. (0.025-cm) increments when water fills and tips a counterbalanced cylinder connected to an electrical switch. Their primary advantage is their good time resolution because data are transmitted every 15 min. Their primary disadvantage is that, if precipitation is received as snow, they tend to record low values (because snow does not flow readily into the measuring cylinder) or delayed values (if water flows into the cylinder only after the snow melts).

The rain gage at Spirit Lake (Fig. 1) was used as the standard for this analysis and was

TABLE 1. SUMMARY OF SHALLOW, EXPLOSION-LIKE SEISMIC EVENTS AND GAS-AND-TEPHRA EMISSIONS, AUGUST 1989–JUNE 1991

Date (local)	Time of onset		Approximate duration of constant shaking	Number of located earthquakes of A or B quality	Emissive activity
	Local	UTM			
8/24/89	2227 PDT	0527	1 hr	26, 0 min–4.5 hr after onset	x
8/25/89	0918 PDT	1618	1 hr	0	N
8/30/89	1758 PDT	0058	35 min	0	x
12/7/89	1609 PST	0009	5 hr	0	T
12/9/89	0601 PST	2201	2 min	0	x
1/6/90	0537 PST	1337	2 hr	0	T,F,B
3/2/90	0034 PST	0834	1 min	0	x
3/2/90	1101 PST	1901	3 min	0	x
4/5/90	0156 PDT	0856	2 min	0	x
4/25/90	0126 PDT	0826	3 hr	1, 2 hr after onset	x
5/8/90	0912 PDT	1612	2 min	1, 15 sec after onset	x
6/7/90	2251 PDT	0751	1 hr	0	x
9/14/90	1950 PDT	0250	3 min	1, 4 min after onset	x
9/24/90	1652 PDT	2352	>3 hr	8, 2–7 min after onset	N
10/15/90	1224 PDT	1924	4 min	1, 1 hr after onset	x
10/25/90	0639 PST	1339	>3 hr	5, 0–22 min after onset	x
10/26/90	0003 PST	0703	4 hr	0	x
11/5/90	0207 PST	1007	1 hr	2, 50 min and 2.5 hr after onset	P,T,F,B
11/14/90	2341 PST	0741	4 min	1, 3 min after onset	x
11/20/90	1058 PST	1858	2 min	5, 0–35 min after onset	x
11/25/90	1245 PST	2045	2 min	0	x
11/28/90	1921 PST	0321	2 min	0	x
12/20/90	1259 PST	2059	3 hr	>60, 1.4 hr–14 days after onset	P,T
12/23/90	1115 PST	1915	1 hr	included in above set	N
1/5/91	2146 PST	0546	3 min	0	x
2/5/91	0747 PST	1547	40 min	0	P,T,F,B
2/14/91	0524 PST	1324	4 hr	0	T,F
6/18/91	0608 PDT	1308	5 min	0	N

Note: >, signal dies out too gradually to estimate exact duration; N, confirmed, no steam or tephra emission; T, recognized tephra deposit; P, visible plume; F, flowage deposit; B, ballistic blocks; x, crater could not be observed to verify emission of steam or tephra during event, but later visits found no new tephra.

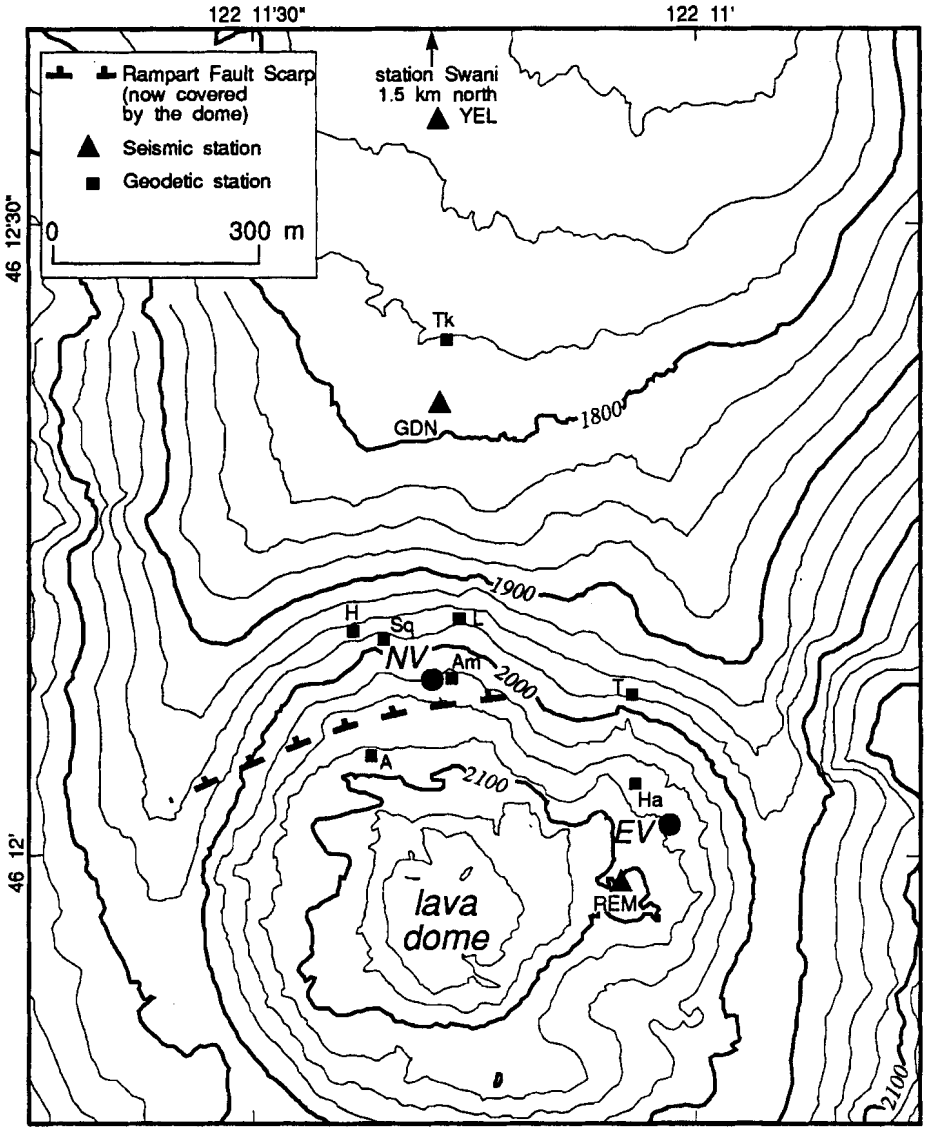

Figure 3. Map of the Mount St. Helens crater (from 1988) showing the locations of vents, seismic stations, geodetic stations, and the Rampart fault scarp. NV, north vent; EV, east vent; A, geodetic station Ansel; Am, Amos 3; H, Hoser; Ha, Harold; L, Luther; S, Squab; T, Tiki; Tk, Tinker. Contour elevations in meters.

checked against gages at Castle Lake (Fig. 1) and Muddy River, 20 km southeast of the crater. Nearly all storms recorded at Muddy River (365-m elevation) or Castle Lake (795 m) were also recorded at Spirit Lake (1,058 m) in spite of the elevation difference, suggesting either that most precipitation at Spirit Lake was rain or that the falling snow melted quickly enough to be recorded.

The timing of storms at Spirit Lake, and of shallow, explosion-like seismic events, is shown in Figure 5. As suspected, all six confirmed emission events closely followed major storms. Most occurred only a few hours after the end of precipitation. The longest delay between the end of a storm and the onset of an emission is 68 hr, prior to the 7 December 1989 event. The correlation between seismic events that were not confirmably associated with emission of gas or tephra is less clear. Those that occurred in May, June, October, and November of 1990 generally followed storms, but those in August 1989 and September 1990 did not.

To estimate the likelihood that the correlation between precipitation and emissions is fortuitous, I use two types of probability tests. The first involves calculating the simple binomial probability that a given number of emission events fortuitously followed a given period of precipitation. As an example, consider the fact that five of six confirmed emissions were preceded by at least 4 cm of precipitation during a 96-h period. What is the probability that this would happen, assuming that emission events occur randomly with respect to storms? Within the time period from 16 August 1989 until 30 June 1991 (a total of 683 days), 100 days (y in Table 2) were preceded by 4 days with at least 4 cm of total precipitation. Given the occurrence of an emission event, the probability (p) that it would take place on one of these days is 100/683 = .1464. The probability that five of the six events would take place on such days is shown in the equation:

$$P(r;n;p) = \frac{p^r(1-p)^{(n-r)}n!}{r!\,(n-r)!} = \frac{(.1464)^5(.8536)^1\,(6!)}{(5!)(1!)} = .0003$$

where r is the number of events that took place after a 4-day period of >4 cm of precipitation, and n is the total number of events.

Table 2 gives the results of similar calculations for time periods ranging from 4 to 15 days and for precipitation ranging from 1 to 15 cm. Groups include (1) all 28 shallow, explosion-like seismic events; (2) confirmed emissions; (3) events that confirmably did not produce emissions; and (4) events where concurrent observations could not confirm the presence or absence of an emission, but where later visits found no new tephra ("remainder of events"). For the "all events" category and for the confirmed emissions, probabilities are frequently less than 0.01 and occasionally less than 0.001 that their timing relative to storms was fortuitous. Confirmed non-emissions give consistently high probabilities, whereas for the "remainder of events," probabilities are frequently less than 0.05 and occasionally less than 0.01.

Binomial probability calculations are intuitively understandable, but they suffer the disadvantage that one must arbitrarily choose a value of precipitation and calculate a probability just for that chosen value. It seems more appropriate to ask, without assigning arbitrary thresholds, whether the overall amount of precipitation preceding these events differs significantly from the amount that one would normally expect in a similar time period. The test employed to address such a question is known as the one-sided, one-sample Kolmogorov test for goodness of

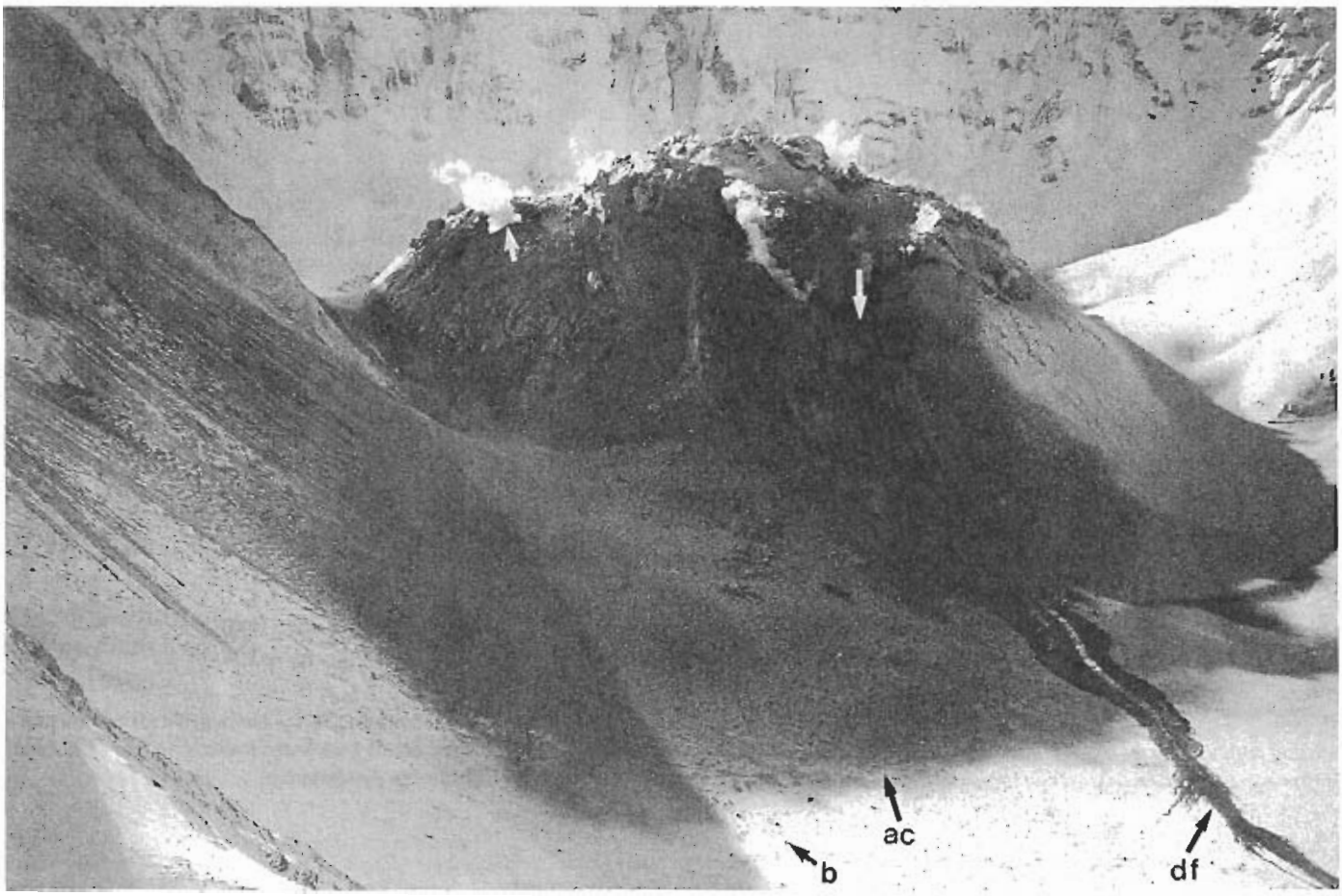

Figure 4. Mount St. Helens lava dome after the emission of 5 February 1991. Debris was apparently ejected from both the north vent (long white arrow) and east vent (short white arrow). Large ballistic blocks (b) and an ash cloud deposit (ac) originated from the north vent; flood and debris-flow deposits (df) originated from the area around the north vent. Photo by R. B. Waitt, 5 February 1991.

fit (Conover, 1971). The Kolmogorov test is similar to the chi squared test in that it involves examining a sample of some population of data (in this case, precipitation preceding emissions) in order to test the hypothesis that the distribution of this sample follows some specified distribution (in this case, the normal for precipitation at this location). Our null hypothesis in this case is that the precipitation preceding emissions was not significantly greater than normal. For this study, the Kolmogorov test is more appropriate than the chi squared test for two reasons. First, the Kolmogorov test does not assume that the data under examination follow a normal Gaussian distribution. This is especially important, because the distribution curve for precipitation over a given time period is not Gaussian. Second, the Kolmogorov test gives exact or conservative probabilities even for small sample populations, whereas the chi squared test assumes that the sample population is large enough to provide a good approximation of the test statistic.

The test is utilized as follows. First, an empirical distribution curve is constructed (the light gage solid line in Fig. 6) for precipitation in a given time period (in this case, 96 hr) preceding confirmed emissions. This curve gives the fraction of all emissions (on the y axis) that were preceded by precipitation of a given amount or less (on the x axis). It is compared with a similar curve representing 4-day precipitation preceding each of the 683 days from 16 August 1989 to 30 June 1991 (the heavy solid line). If the timing of emissions were independent of the precipitation that preceded them, then the two curves should approximately follow each other. The curve for emissions in fact lies well below that for normal precipitation. To determine the probability (α) that the difference in these curves is due to random sampling, we find the largest vertical difference between the two curves where the normal precipitation curve is above the curve for precipitation preceding emissions (K-S, Fig. 6). Using this value (.8501, known as the Kolmogorov-Smirnov Statistic) and the size of the sample population (6 emissions), equations in Birnbaum and Tingey (1951) give the probability as about 1×10^{-5}.

Table 3 presents results of similar analyses for time intervals from 2 to 15 days, for the same four populations of events considered in the binomial probability calculations. The results are not very different from those for the more intuitive but less statistically appropriate binomial probability calculations. If one arbitrarily considers results with $\alpha \leq 0.05$ to be significant, the confirmed emissions results are highly significant, as are the results for the 28 events as a whole. The non-emission events show no significant deviation at all, whereas the results for the "remainder of events" category are rather ambiguous. The deviations for all groups are most significant over time periods of 4 to 6 days but can still be significant for periods as short as 2 days (for confirmed emissions and "all events") or as long as 15 days (for all but non-emission events). The good correlation between rain-

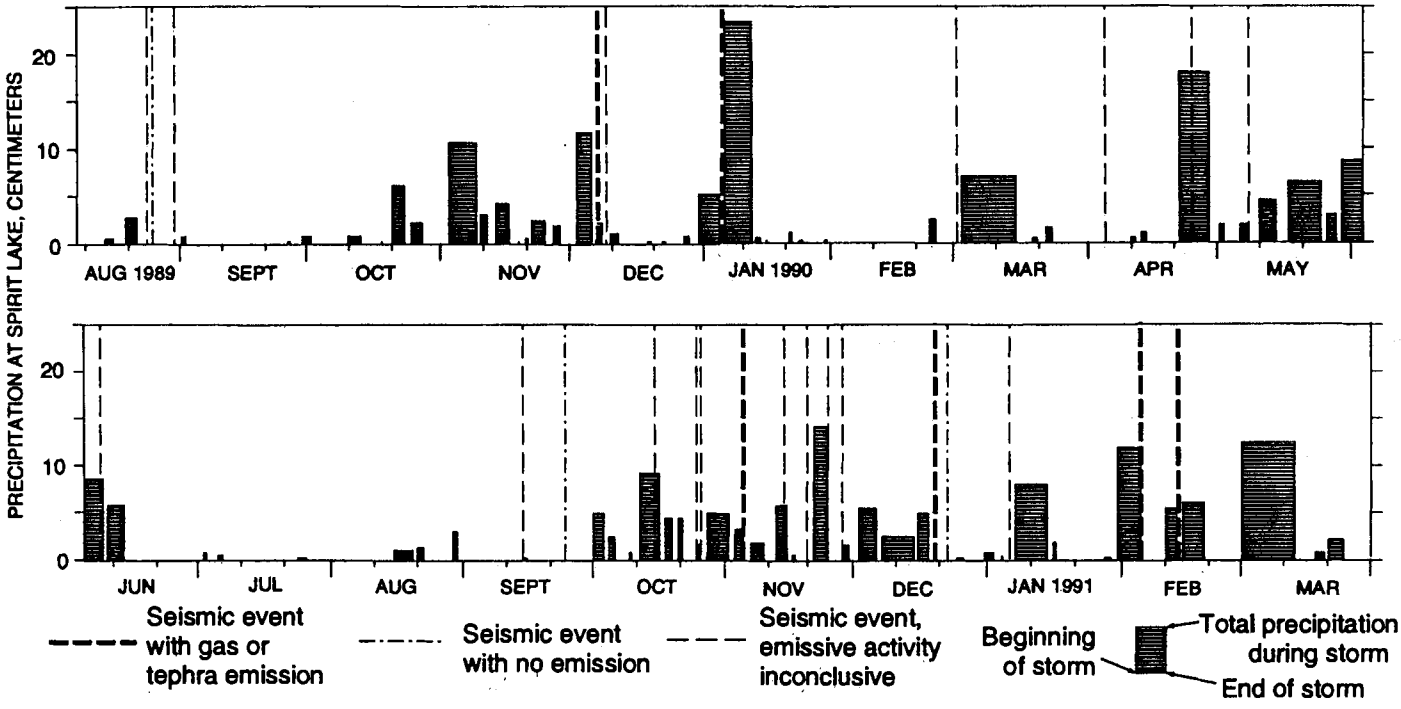

Figure 5. Timing of storms at Spirit Lake and of shallow, explosion-like seismic events. Small tick marks on the horizontal axis represent the 10th and 20th of each month. The right and left side of each box represents the exact time of the first and last recorded precipitation in each storm. Storms are distinguished from one another if they are separated by at least 24 hr with no measurable precipitation.

fall and seismicity over such long periods indicates that shallow, explosion-like seismic events not only tend to follow individual storms, but can also be brought on by the effect of storm sequences lasting weeks.

One could perhaps argue that the test for emission events gives a significant result because we are comparing precipitation before these events, which took place at the rainiest time of the year, with the entire two-year precipitation record, both rainy season and dry season. Table 3 also gives 4- and 6-day results comparing the precipitation prior to emissions with just the rain-gage records for the months November through February. A similar comparison was made using other seismic events; to be consistent, however, only those that took place between November and February were included in the comparison. The results do not differ very much from previous ones.

The fact that most shallow, explosion-like seismic events follow within hours to, at most, days after storms indicates that the triggering mechanism must be shallow, probably within the dome itself. It would seem surprising that seismic data, described in the next section, suggest a source of gas that is well below the dome.

SEISMIC ACTIVITY: THE EVIDENCE FOR A DEEP SOURCE

A deep gas source is indicated by two lines of evidence: the locations of shallow, explosion-like seismic events; and an increase in seismicity at greater depth.

More than 61 earthquakes were located by personnel at the Cascades Volcano Observatory during shallow, explosion-like seismic events. Most locatable earthquakes (the small black squares in Fig. 7) were small bursts of energy that occurred in the tails of the seismic signals. They cluster in an area that has been a locus of nonmagmatic earthquakes since 1980 (Weaver and others, 1987) and may have been a conduit for magmatic gas transport preceding a violent 19 March 1982 eruption (Weaver and others, 1983). Three locations (the large, hollow squares) record onsets to shallow, explosion-like seismic events, on 24 August 1989, 25 October 1990, and 20 November 1990. These are highly significant because they indicate the source depth of the seismicity. Solutions were located using 7 to 12 stations around the mountain (Fig. 1) including 1 to 3 in the crater. They give low RMS residuals (0.05–0.11 s), and yield depths of 1.44 km to 2.10 km with standard errors of 0.3 km or less. Using a technique developed by Endo and others (1990), the depth was checked independently of the velocity model used in the above solutions by taking the difference in times of arrival at stations GDN and REM, along a radial path from the conduit. For the 24 August 1989 event (the only one where both stations were in operation), the time difference (0.12 s with an uncertainty of ±0.01 s in each pick) is less than half what one would expect for a source within the dome but is consistent with a source depth of 1–2 km. It is therefore very unlikely that these locations were near the surface.

The depth of these onsets appears inconsistent with the inference, derived from the association with storms, that the shallow, explosion-like seismic events are near-surface phenomena. It is important to note that none of the three located events followed storms, nor did they produce confirmable evidence of gas or tephra emission. Do the located events represent a different type of seismicity from those associated with storms? The facts that the seismic signatures for both events (the located, deep ones and the storm-related, presumably shallow ones) are indistinguishable from one another, and that both events took

TABLE 2. PROBABILITY VALUES FOR THE FORTUITOUS OCCURRENCE OF SHALLOW, EXPLOSION-LIKE SEISMICITY FOLLOWING A GIVEN AMOUNT OF PRECIPITATION IN A GIVEN TIME PERIOD

		Centimeters precipitation					
4-day period		1	2	4	6	8	n
	y	327	214	100	45	20	
	p (=y/683)	0.4788	0.3133	0.1464	0.0659	0.0293	
All events	r	19	14	9	5	4	28
	P(r;n;p)	0.0164	0.0183	0.0105	0.0254	0.0074	
Emissions	r	6	6	5	2	2	6
	P(r;n;p)	0.0120	0.0009	0.0003	0.0496	0.0114	
Non-emissions	r	1	0	0	0	0	4
	P(r;n;p)	0.2712	0.2223	0.5309	0.7614	0.8879	
Remainder of events	r	12	8	4	2	1	18
	P(r;n;p)	0.0540	0.0947	0.1533	0.2232	0.3180	
6-day period		2	4	6	8	10	n
	y	316	176	93	50	25	
	p (=y/683)	0.4627	0.2577	0.1362	0.0732	0.0366	
All events	r	20	16	10	6	4	28
	P(r;n;p)	0.0044	0.0003	0.0021	0.0109	0.0150	
Emissions	r	6	6	3	2	2	6
	P(r;n;p)	0.0098	0.0003	0.0325	0.0593	0.0173	
Non-emissions	r	3	1	0	0	0	4
	P(r;n;p)	0.2129	0.4216	0.5568	0.7378	0.8614	
Remainder of events	r	11	9	7	4	2	18
	P(r;n;p)	0.0856	0.0167	0.0055	0.0303	0.1129	
10-day period		2	4	6	8	10	n
	y	431	297	221	139	81	
	p (=y/683)	0.6310	0.4348	0.3236	0.2035	0.1186	
All events	r	24	19	15	11	7	28
	P(r;n;p)	0.0060	0.0055	0.0104	0.0111	0.0276	
Emissions	r	6	6	5	4	2	6
	P(r;n;p)	0.0631	0.0068	0.0144	0.0163	0.1273	
Non-emissions	r	3	2	1	0	0	4
	P(r;n;p)	0.3709	0.3624	0.4006	0.4025	0.6035	
Remainder of events	r	15	11	10	7	5	18
	P(r;n;p)	0.0411	0.0616	0.0241	0.0377	0.0389	
15-day period		2	4	6	10	15	n
	y	497	389	314	200	76	
	p (=y/683)	0.7266	0.5687	0.4591	0.2924	0.1111	
All events	r	24	19	18	13	9	28
	P(r;n;p)	0.0537	0.0786	0.0231	0.0239	0.0019	
Emissions	r	6	6	6	4	2	6
	P(r;n;p)	0.1472	0.0338	0.0094	0.0549	0.1156	
Non-emissions	r	3	2	1	0	0	4
	P(r;n;p)	0.3709	0.3624	0.4006	0.4025	0.6035	
Remainder of events	r	15	11	11	9	7	18
	P(r;n;p)	0.1385	0.1778	0.0823	0.0338	0.0018	

place in 1989–1991 and not before or after, lead one to believe that they do not. A more likely possibility is that they all have the same cause (that is, gas transport) but took place at depths ranging from near the surface to at least 1–2 km. Confirmed emissions may represent a subset at the shallow end of this range, but confirmed non-emissions may be disproportionately represented by deeper members. In any case, the fact that some originate well below the dome leads one to conclude that the source of gas is not within the dome or anywhere near the surface. It is deep enough to be derived from the magmatic conduit or from the magma chamber.

The deep seismicity at Mount St. Helens has been studied by Moran (in press). Moran found that background seismicity between ~2- and 9-km depth began to increase from an average of ~2 locatable earthquakes per month in early 1987 to 90 per month in the first half of 1990 (Fig. 8) but then declined to ~20 per month in the latter half of 1992. The peak in background level coincided remarkably well with the early part of the period of shallow, explosion-like seismicity. This increase is unprecedented in the post–1980 earthquake record and differs from typical precursory activity in two respects: (1) it took place over years, rather than weeks or months as was typical for precursors to eruptions of the early 1980s; and (2) most earthquakes between 1987 and 1990 were below 3 km depth, whereas shallower depths were associated with all precursory records except a March 1982 explosion (Weaver and others, 1983; Moran, in press).

The increase in deep seismicity since 1987 alone does not necessarily indicate that the gas source to the emissions was deep; however, when combined with the onset locations, the story for a deep source is difficult to dismiss. New, small, deep intrusions may have been a source of gas, although there is no evidence (other than the seismic increase) of new intrusions. An alternative possibility, for which there is more evidence, is that gas came directly from the crystallizing conduit.

DEEP-SOURCE MECHANISMS

The crystallization of magma in the Mount St. Helens eruptive conduit and the accompanying exsolution of volatile species has been the subject of at least two previous papers (Cashman, 1988, 1992). Based on examination of dome rock samples, Cashman (1988, 1992) estimated that crystallization of plagioclase microphenocrysts by cooling of magma in the eruptive conduit averaged ~0.1 vol%/month from early 1981 to 1986. The amount of gas exsolved during crystallization, Cashman (1988) argued, could cause episodes of second boiling regularly enough to trigger the dome-building eruptions. By 1986, crystals made up some 60% of the total rock volume. The high crystallinity increased magma viscosity greatly and was probably a major factor in preventing further eruptions (Cashman, 1988).

Since the last dome-building eruption, magma in the conduit has presumably continued to cool, but gas has not been allowed to escape during dome-building episodes as before. If crystallization continued at the 1981–1986 rate after dome-building eruptions ended, the crystal content would have increased by approximately another 4.5% of the total magma volume (that is, volume of melt plus crystals) by mid–1990. Assuming

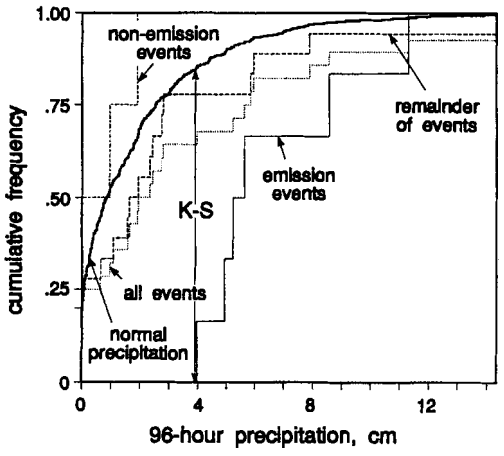

Figure 6. Cumulative distribution of 96-hr precipitation values recorded at Spirit Lake: for all precipitation recorded, 8/16/89–6/30/91 (heavy solid line); for precipitation preceding confirmed emission events (light solid line); for precipitation preceding non-emission seismic events (long-dashed, short-dashed line); for precipitation preceding seismic events which are neither confirmed emission events nor confirmed non-emission events (long-dashed line); and for precipitation preceding all shallow, explosion-like seismic events (dotted line).

that the magma between 2- and 7-km depth was saturated at ~3–4.5 wt% water (~3% at shallow depth, 4.5% at greater depth), the crystallization of an additional 4.5 vol% plagioclase would have released ~3–5 kg water per cubic meter of melt, or 4×10^7 to 3×10^8 kg total water from a conduit of 30- to 60-m radius (Pallister and others, 1992).

Would this amount of gas have been sufficient to drive the emissions? Some simple energetics calculations suggest that it may have. The internal energy (above that of liquid water at 1 atm, 100 °C) of this water vapor, released from the conduit at magmatic temperature (870–930 °C; Rutherford and others, 1985; Cashman, 1992) and subsurface pressures (~50–175 MPa), would have been approximately 1×10^{14} to 1×10^{15} joules (Haar and others, 1984). Even at temperatures and pressures appropriate to the interior or the dome (4–5 MPa, ~300–600 °C), the available energy would have been essentially the same: 1×10^{14} to 1×10^{15} joules.

The energy required to produce the emissions can be made only approximately, but data are available to make an order of magnitude estimate for one of the more powerful ones. The average ejection velocity (v = 40–80 m/s) from the 5 November 1990 event, taken from ballistic studies mentioned above, combined with estimates of the erupted mass (m) calculated from the volume of the crater ($1.2–2.4 \times 10^3$ m^3) and an assumed *in situ* rock density of ~2,000 kg/m^3, suggest a kinetic energy of erupted debris ($= 0.5\ m\ v^2$) on the order 2×10^9 to 1.5×10^{10} joules. Based on ratios of kinetic to total energy of steam eruptions elsewhere (White, 1955; Le Guern and others, 1980), the total energy of this event may have been two to three orders of magnitude greater, perhaps 10^{11}–10^{13} joules. This is one to three orders of magnitude less than the energy available in the exsolved gas. The total energy release for all emissions may have ranged from about the same order of magnitude as the energy contained in the exsolved gas, to a few orders of magnitude less.

SPECULATIONS ON A SHALLOW TRIGGER

Given the current level of knowledge, it is impossible to confidently identify a causal mechanism for the association between emissions and precipitation. The fact that gas was released during explosive episodes rather than continuously suggests that it was contained beneath a shallow, impermeable cap, probably within the dome, that breached during storms. What was that cap and how was it breached? A bit of background on the local geology may shed some light on this question.

The dome's north flank consists of three rubbly exogenous lobes, below which lies a thick section of lava emplaced endogenously during at least three periods of dome growth (Fig. 9). At the base of the dome, there are rubbly zones that may have either dissipated or stored gas. Magnetic field strength measurements indicate that the dome's interior, including probably the inner dome below the North and East vents, is well above the magnetization temperature (~375–600 °C) and could still deform viscously. Above the viscous interior, the entire dome has been fracturing and disintegrating as it cools. Massive rock outcrops and spires many meters high on the dome's surface have crumbled since 1986 to piles of rubble. Aprons of debris of have grown as unstable talus rolls and avalanches to the dome's base. The North Vent itself formed within a previously unrecognized, arcuate pull-apart feature that resembled the head scarp of a landslide (D. Dzurisin, 1993, oral commun.), and a geodetic station (Luther, Fig. 10) subsequently placed below the North Vent showed greater downslope movement than nearby stations before it was destroyed in the next explosion. The final three emissions from the North Vent were accompanied by an unprecedented removal of 8×10^5 m^3 of debris from the dome's north flank (Fig. 9), mostly by avalanches and rockslides. This is at least an order of magnitude more debris than had been removed from any part of the dome since 1986.

Magnetic field strength measurements (Dzurisin and others, 1990) also show that the solidified carapace around the viscous interior has thickened at an average rate of 0.03 ± .01 m/day since the end of dome growth. In accord with observations of Kilauea Iki lava lake in Hawaii (Hardee, 1980), Dzurisin and others (1990) inferred that thickening of the carapace is accompanied by downward propagation of cooling fractures. Both Hardee (1980) and Dzurisin (1990)

TABLE 3. PROBABILITIES THAT PRECIPITATION VALUES RECORDED IN THE DAYS PRECEDING SEISMIC AND EMISSION EVENTS WAS FORTUITOUSLY GREATER THAN NORMAL

	Compared with total precipitation record, 8/16/89–6/15/91						Compared with record from November through February		
Probability	n*	2-day	4-day	6-day	10-day	15-day	n*	4-day	6-day
All events	28	0.031	0.029	1.1E-03	0.011	0.025	13	0.0179	3.5E-03
Confirmed emissions	6	0.011	1.2E-05	2.4E-04	2.2E-03	4.4E-03	6	1.9E-04	2.5E-03
Non-emission events	4	0.191	0.994	0.257	0.609	0.800	1	0.8723	0.3991
Remainder of events	18	0.102	0.170	0.069	0.078	0.037	6	0.1718	0.0394
K-S statistic									
All events	28	0.2421	0.2446	0.3392	0.2768	0.2505	13	0.3774	0.447
Confirmed emissions	6	0.5730	0.8477	0.7540	0.6603	0.6237	6	0.7617	0.6524
Non-emission events	4	0.4181	0.0066	0.3781	0.2171	0.1365	1	0.1277	0.6009
Remainder of events	18	0.2424	0.2129	0.2628	0.2568	0.2996	6	0.3574	0.4864

*n = population size.

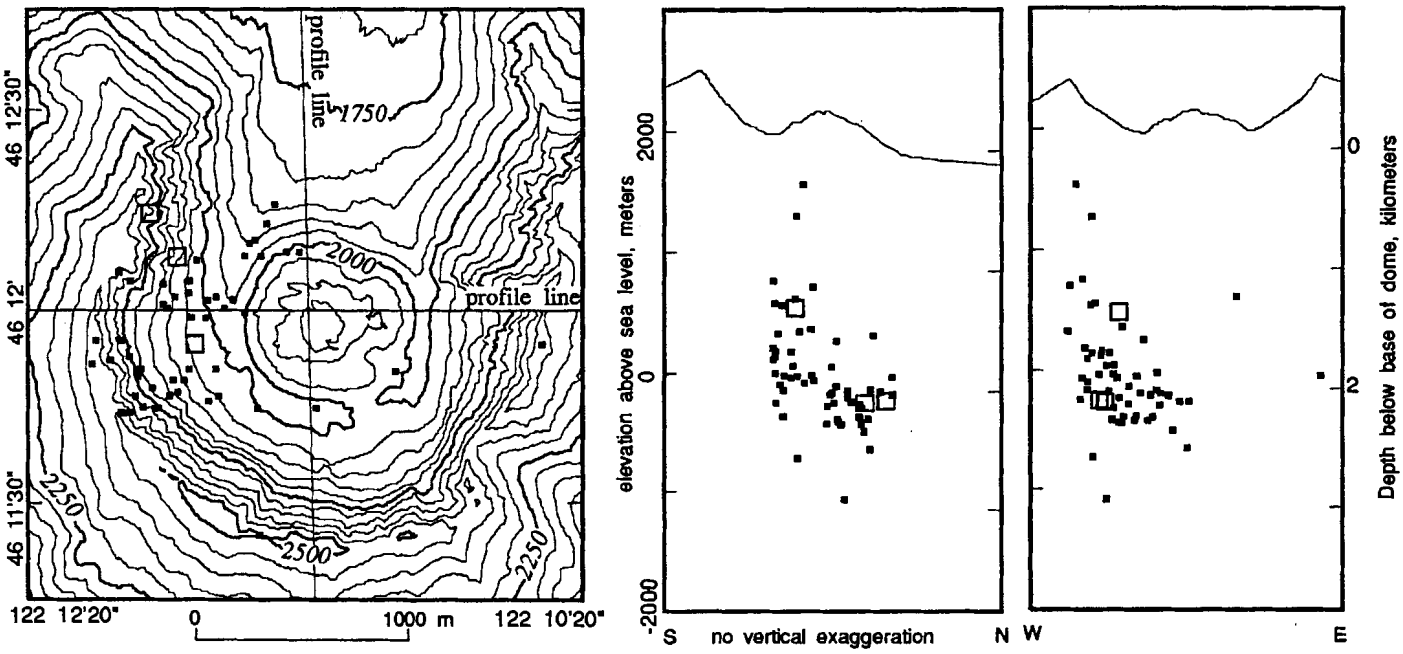

Figure 7. Location of earthquakes that occurred during shallow, explosion-like seismic events and that meet U.S. Geological Survey, Cascades Volcano Observatory requirements for "A" or "B" quality. Large hollow squares represent onsets of shallow, explosion-like seismic events. Small black squares are earthquakes that occurred after event onsets. Standard errors in horizontal and vertical locations are 0.1–0.6 km and 0.1–0.3 km, respectively. Only earthquakes that took place less than 24 hr after the 20 December 1990 event are plotted to prevent those events from dominating the pattern.

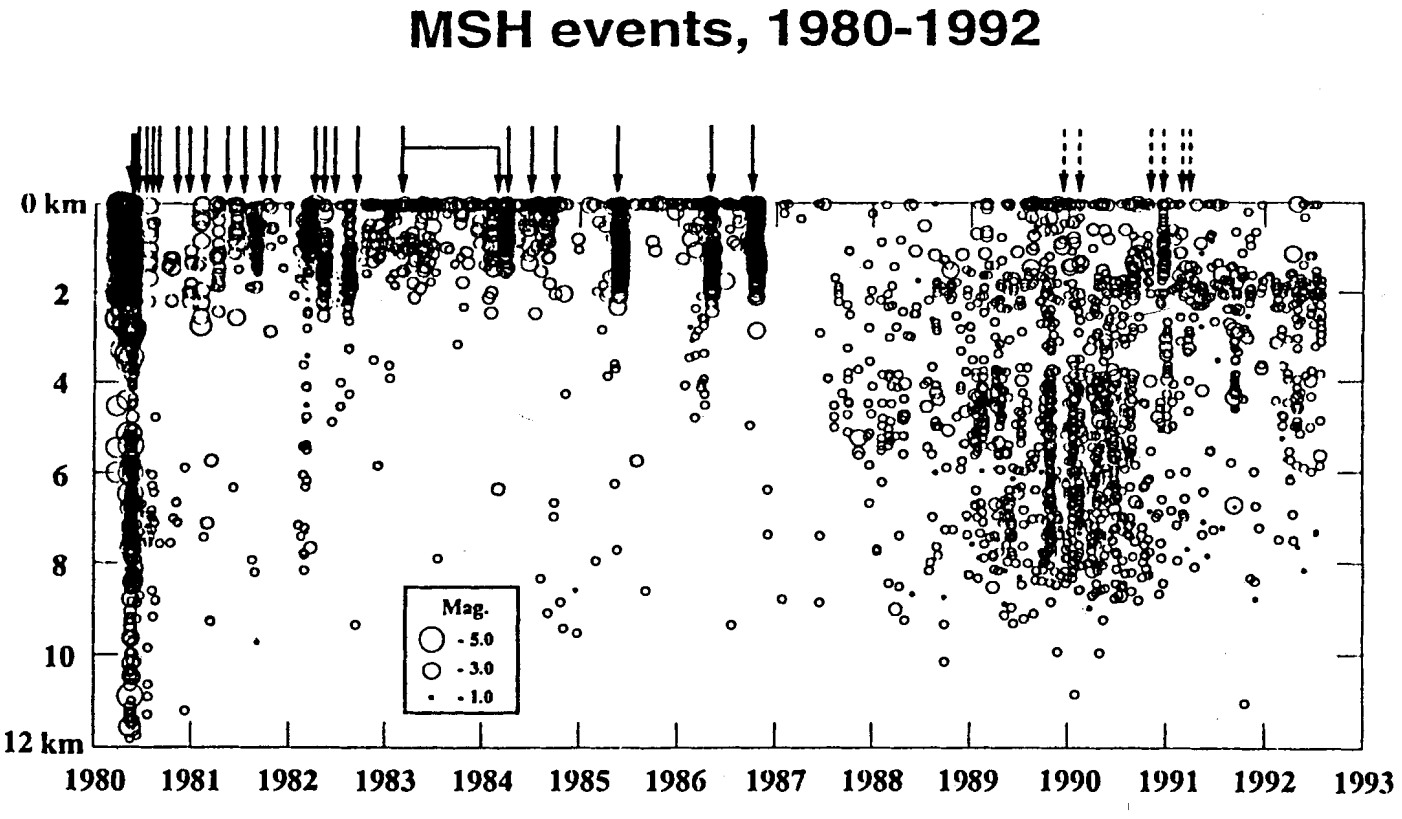

Figure 8. Time versus depth plot of all earthquakes below Mount St. Helens located by the University of Washington, that meet the University of Washington's quality "BB" standard and occurred between 1980 and July 1992. Solid arrows indicate the onset time of confirmed eruptions. Dashed arrows between 1989 and 1991 correspond to six confirmed steam explosions. Note that 0 km corresponds to mean station elevation, ~1 km below the crater floor (in contrast to locations plotted in Fig. 7). Figure taken from Moran (in press).

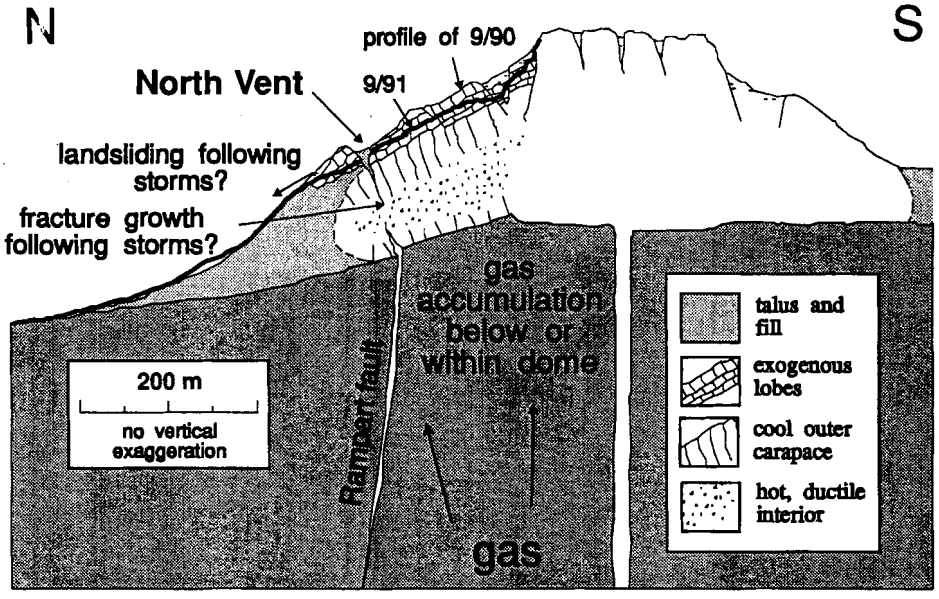

Figure 9. Schematic north-south cross section through the Mount St. Helens lava dome illustrating the mechanisms suggested for explosive release of magmatic gas following storms. Internal structures in the central and southern portions of the dome are not included in this figure. Location of exogenous lava lobes on the north side of the lava dome are taken from air photos and from maps in Swanson and others (1987). Thickness of exogenous lobes is taken from photogrammetric measurements and from field observations. Thickness of convectively cooled upper carapace on the north side of the dome is estimated by integrating Dzurisin and others' (1990) calculated average rate of thickening of the dome's magnetic carapace (0.03 ± 0.01 m/d) from late 1984 (the time of last lava extrusion on the north side) until 1990. Profiles were done using photogrammetry from air photos taken in September 1990 and September 1991.

found that atmospheric precipitation is dominant in determining the rate of cooling of these lava bodies. At Kilauea Iki, the heating to 100 °C and vaporization of all water that fell on the lava lake accounts for about two-thirds of the cooling rate. At Mount St. Helens, it accounts for one-third to one-half. The rate of cooling at Mount St. Helens has been found to be several tens of percent higher during wet seasons than during dry seasons and, most importantly, exhibits jumps during individual storms (D. Dzurisin, 1992, oral commun.).

One could imagine that accelerated fracture growth and disaggregation of the dome during storms may have opened passageways between gas-charged regions and the surface. In the North Vent area, slope instability caused by the added weight of water, increases in pore pressure, rapid expansion of steam, or reduction of strength by thermal fracturing could also have exposed regions of pressurized gas. In the East Vent area, no significant amount of mass wasting took place during the explosions, although dome disintegration and fracturing were clearly evident from air photos of this area and presumably were also taking place in the subsurface.

In the dome's interior, propagation of cooling fractures through the viscous center of the dome during storms could conceivably have released gas from the base of the dome to the surface. Calculations of average fracture growth rate suggest that the cooling fractures probably extended to somewhere near the center of the endogenous lobe below the North Vent by late 1989 (Fig. 9) and could have connected with fractures growing up from the base of the dome. If the fracture growth rate during storms was several times the average rate, cooling fractures would have propagated only a few centimeters to several tens of centimeters over the duration of a storm, and perhaps to meters over the course of several storms. If this growth occurred in an area that was loaded by topographic stresses or pressure from underlying gases, however, the potential growth of fractures would have been unlimited. Stable or subcritical crack growth could have given way to unstable crack growth that propagated completely through the dome. Ductile flow could have annealed the fractures between emission events, although progressive cooling would ultimately have terminated the annealing process.

At least one other lava dome, at Merapi Volcano, Indonesia, produces large flank failures during storms, apparently also by fracture and disaggregation. This dome first appeared in January 1992 and extruded onto the volcano's steeply sloping (30°–40°) flank during the first half of that year (Smithsonian Institution, 1992). Since January 1992, more than 45 pyroclastic flows have been triggered by dome-collapse events (as of April 1993); more than 90% of these have taken place on days of rainfall. Members of the Merapi Volcano Observatory (S. Bronto, 1993, written commun.) noted that, during rainstorms, blocks on the dome's flank are dislodged by pressure from expanding steam, and the dome eventually detaches along a surface that propagates all the way through the dome's massive interior.

The more moderate slope beneath the Mount St. Helens dome and its cooler temperature mean that fracture growth and disaggregation are probably less extensive at Mount St. Helens during each storm than at Merapi. Unlike Merapi, the primary force driving fracture growth at Mount St. Helens was probably internal gas pressure. As gas pressures increased in the dome, the internal seal between regions of high pressure and low pressure were subjected to greater stress until small perturbations, caused by water infiltration, triggered complete failure. These explosions probably would have taken place with or without precipitation, although the storms apparently forced the explosions to occur slightly sooner than they would otherwise have.

CLOSING REMARKS

The emissions and shallow, explosion-like seismicity have discontinued for the present, although magma in the conduit is presumably continuing to crystallize. One can imagine two possible explanations for the discontinuation: (1) gas pressures that built up during 1986–1989 subsided during 1989–1991 and are now building up again, in which case we might expect renewed emissions and seismicity in the near future. Alternatively, (2) pathways have been opened that allow continuous slow escape of magmatic gas, in which case renewed emissions would be unlikely. These alternatives can be tested by future observations.

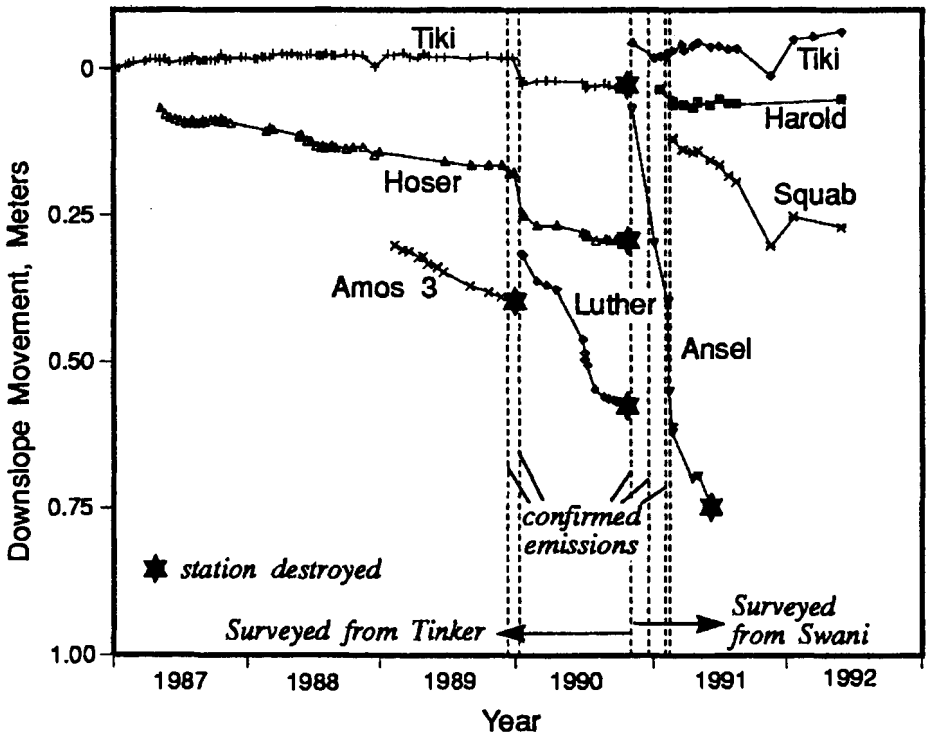

Figure 10. Changes in slope distance versus time, measured from points north of the dome to geodetic stations on the north side of the dome. Locations of geodetic stations are shown in Figure 3. Before 5 November 1990, stations were surveyed from the point Tinker, near the north base of the dome. After 5 November 1990, they were surveyed from a station (Swani) ~1.8 km north of the dome.

ACKNOWLEDGMENTS

Information in this report was collected by many workers at the U.S. Geological Survey in Vancouver and at the Geophysics Program, University of Washington. Field observations were provided by Richard Waitt, Edward Wolfe, Donald Swanson, Daniel Dzurisin, and Jack Kleinman. Terry Gerlach proposed that the recent events may be related to second boiling. Bobbie Myers and Chris Jonientz-Trisler (with help from others at the University of Washington) identified the shallow, explosion-like seismic events. Earthquake locations were determined by Gloria Smith, and helpful reviews of this paper were made by John Eichelberger, Steve Ingebritsen, Donald Swanson, and Elliot Endo.

REFERENCES CITED

Birnbaum, Z. W., and Tingey, F. H., 1951, One-sided confidence contours for probability distribution functions: Annals of Mathematical Statistics, v. 22, p. 592–596.

Cashman, K. V., 1988, Crystallization of Mount St. Helens 1980–1986 dacite: A quantitative textural approach: Bulletin of Volcanology, v. 50, p. 194–209.

Cashman, K. V., 1992, Groundmass crystallization of Mount St. Helens dacite, 1980–1986: A tool for interpreting shallow magmatic processes: Contributions to Mineralogy and Petrology, v. 109, p. 431–449.

Chadwick, W. W., and Swanson, D. A., 1989, Thrust faults and related structures in the crater floor of Mount St. Helens volcano, Washington: Geological Society of America Bulletin, v. 101, p. 1507–1519.

Chadwick, W. W., Swanson, D. A., Iwatsubo, E. Y., Heliker, C. C., and Leighley, T. A., 1983, Deformation monitoring at Mount St. Helens in 1981 and 1982: Science, v. 221, p. 1378–1380.

Chouet, B. A., Page, R. A., Stephens, C. D., and Lahr, J. C., in press, Precursory swarms of long-period events at Redoubt volcano (1989–1990), Alaska: Their origin and use as a forecasting tool: Journal of Volcanology and Geothermal Research.

Conover, W. J., 1971, Practical nonparametric statistics: New York, John Wiley and Sons, 462 p.

DeGraff, J. M., and Aydin, A., 1987, Surface morphology of columnar joints and its significance to mechanics and direction of joint growth: Geological Society of America Bulletin, v. 99, p. 605–617.

Dzurisin, D., Westphal, J. A., and Johnson, D. J., 1983, Eruption prediction aided by electronic tiltmeter data at Mount St. Helens: Science, v. 221, p. 1381–1382.

Dzurisin, D., Denlinger, R. P., and Rosenbaum, J., 1990, Cooling rate and thermal structure determined from progressive magnetization of the dacite dome at Mount St. Helens, Washington: Journal of Geophysical Research, v. 95, p. 2763–2780.

Endo, E. T., Dzurisin, D., and Swanson, D. A., 1990, Geophysical and observational constraints for ascent rates of dacitic magma at Mount St. Helens: New York, John Wiley and Sons, p. 317–334.

Haar, L., Gallagher, J. S., and Kell, G. S., 1984, NBS/NRC steam tables: New York, Hemisphere Publishing Corporation, 320 p.

Hardee, H. C., 1980, Solidification in Kilauea Iki Lava Lake: Journal of Volcanology and Geothermal Research, v. 7, p. 211–233.

Jonientz-Trisler, C., Myers, B., and Power, J., 1991, Seismic identification of gas-and-ash explosions at Mount St. Helens: Capabilities, limitations, and regional application, *in* First International Symposium on Volcanic Ash and Airline Safety, Seattle, WA, July 8–12, 1991, Proceedings: U.S. Geological Survey Bulletin 1065: Washington, D.C., U.S. Government Printing Office, p. 26–27.

Kerr, R. A., 1993, Volcanologists ponder a spate of deaths in the line of duty: Science, v. 260, p. 289–290.

Le Guern, F., Bernard, A., and Chevrier, R. M., 1980, Soufriere of Guadeloupe 1976–1977 eruption—Mass and energy transfer and volcanic health hazards: Bulletin Volcanologique, v. 43, p. 578–592.

Lipman, P. W., and Mullineaux, D. R., eds., 1981, The 1980 eruptions of Mount St. Helens, Washington: U.S. Geological Survey Professional Paper 1250: Washington, D.C., U.S. Government Printing Office, 844 p.

Mastin, L. G., 1991, The roles of magma and groundwater in the phreatic eruptions at Inyo Craters, Long Valley Caldera, California: Bulletin of Volcanology, v. 53, p. 579–596.

McBirney, A. R., 1955, Thoughts on the eruption of the Nicaraguan volcano Las Pilas: Bulletin Volcanologique, v. 17, p. 113–117.

Moran, S. C., in press, Seismicity at Mount St. Helens, 1987–1992: Evidence for repressurization of an active magmatic system: Journal of Geophysical Research.

Murray, J. B., 1980, The Bocca Nuova: Its history and possible causes of the September 1979 explosion, *in* Huntington, A. T., Guest, J. E., and Francis, E. H., eds., United Kingdom Research on Mount Etna, 1977–1979: London, England, The Royal Society of London, p. 46–50.

Pallister, J. S., Hoblitt, R. P., Crandell, D. R., and Mullineaux, D. R., 1992, Mount St. Helens a decade after the 1980 eruptions: Magmatic models, chemical cycles, and a revised hazards assessment: Bulletin of Volcanology, v. 54, p. 126–146.

Rutherford, M. J., Sigurdsson, H., Carey, S., and Davis, A., 1985, The May 18, 1980, eruption of Mount St. Helens 1. Melt composition and experimental phase equilibria: Journal of Geophysical Research, v. 90, p. 2929–2947.

Smithsonian Institution, 1992, Merapi (Java): Pyroclastic flows follow earthquakes and rainfall; gas data: Bulletin of the Global Volcanism Network, v. 17, no. 10, p. 3.

Smithsonian Institution, 1993, Guagua Pichincha (Ecuador): Phreatic explosion kills two scientists: Bulletin of the Global Volcanism Network, v. 18, no. 2, p. 2.

Swanson, D. A., Casadevall, T. J., Dzurisin, D., Malone, S. D., Newhall, C. G., and Weaver, C. S., 1983, Predicting eruptions at Mount St. Helens, June 1980 through December 1982: Science, v. 221, p. 1369–1376.

Weaver, C. S., Zollweg, J. E., and Malone, S. D., 1983, Deep earthquakes beneath Mount St. Helens: Evidence for magmatic gas transport?: Science, v. 221, p. 1391–1394.

Weaver, C. S., Grant, W. C., and Shemeta, J. E., 1987, Local crustal extension at Mount St. Helens, Washington: Journal of Geophysical Research, v. 92, p. 10170–10178.

White, D. E., 1955, Violent mud-volcano eruptions of Lake City Hot Springs, northeastern California: Geological Society of America Bulletin, v. 66, p. 1109–1130.

MANUSCRIPT RECEIVED BY THE SOCIETY OCTOBER 19, 1992
REVISED MANUSCRIPT RECEIVED APRIL 21, 1993
MANUSCRIPT ACCEPTED JUNE 22, 1993

Printed in U.S.A.